Peer-reviewed version available at *Cancers* **2019**, *11*, 711; doi:10.3390/cancers11050711

Article

The Novel Thienopyrimidine Derivative, RP-010, Produces Its Efficacy in Prostate Cancer Cells by Inducing the Fragmentation of β-catenin

Haneen Amawi [1,2], Noor Hussein [1], Sai HS Boddu [3,4], Chandrabose Karthikeyan [5,6], Frederick E. Williams [1], Charles R. Ashby Jr. [7], Dayanidhi Raman [8], Piyush Trivedi [5] and Amit K. Tiwari [1,*]

[1] Department of Pharmacology and Experimental Therapeutics, College of Pharmacy & Pharmaceutical Sciences, University of Toledo, OH; haneen.amawi@rockets.utoledo.edu (H.A.); noor.hussein@rockets.utoledo.edu (N.H.); frederick.williams2@utoledo.edu (F.W.)
[2] Department of Pharmacy Practice, Faculty of Pharmacy, Yarmouk University, P.O.BOX 566, Irbid 21163, Jordan; haneen.amawi@yu.edu.jo (H.A)
[3] College of Pharmacy and Health Sciences, Ajman University, UAE; s.boddu@ajman.ac.ae (S.B.)
[4] Department of Pharmacy Practice, College of Pharmacy & Pharmaceutical Sciences, University of Toledo, OH s.boddu@ajman.ac.ae (S.B.)
[5] School of Pharmaceutical Sciences, Rajiv Gandhi Proudyogiki Vishwavidyalaya, Airport Bypass Road, Gandhi Nagar, Bhopal (MP) 462036, India; karthinobel@gmail.com(C.K.); piyushtrivedi304@gmail.com
[6] Department of Pharmacy, Indira Gandhi National Tribal University, Amarkantak, MP, 484887, India; karthinobel@gmail.com (C.K.)
[7] Department of Pharmaceutical Sciences, College of Pharmacy, St. John's University, Queens, NY; cnsratdoc@optonline.net
[8] Department of Cancer Biology, College of Medicine, University of Toledo, OH; dayanidhi.raman@utoledo.edu
* Corresponding Author: amit.tiwari@utoledo.edu; Tel: 419-383-1913; Fax: 419-383-1909

Abstract: Thienopyrimidines are a versatile group of compounds that contain a biologically active pharmacophore and are reported to have anticancer efficacy *in vitro*. Here, we report for the first time, that thieno[3,2-d]pyrimidine - based compounds, the RP series, have efficacy in prostate cancer cells. The lead compound, RP-010, was efficacious in PC3 and DU-145 prostate cancer (PC) cells (IC_{50}< 1μM). The cytotoxicity of RP-010 was significantly lower in normal cells. RP-010 (0.5, 1, 2, and 4 μM) arrested prostate cancer cells in the G2 phase of the cell cycle, induced mitotic catastrophe and apoptotic signaling in both PC cell lines. Mechanistic studies suggested that RP-010 (1 and 2 μM) inhibits the wingless-type MMTV (Wnt)/β-catenin signaling pathway, mainly by inducing β-catenin fragmentation, while down regulating important proteins in the pathway, i.e. LRP-6, DVL3, and c-Myc. Interestingly, RP-010 (1 and 2 μM) induced the nuclear translocation of the negative feedback proteins, Naked 1 and Naked 2, in the signaling pathway. In addition, RP-010 (0.5, 1, 2 and 4 μM) significantly decreased the migration and invasiveness of PC cells *in vitro*. Finally, RP-010 did not produce significant toxic effects in zebrafish at concentrations up to 6 μM. In conclusion, RP-010 may be a promising anticancer compound for metastatic prostate cancer and it did not produce overt toxicity in an *in vivo* zebrafish model. Future mechanistic and efficacy studies are needed *in vivo* to optimize the lead compound RP-010 for clinical use.

Keywords: Thienopyrimidines; RP-010; Prostate cancer; Metastasis; Wnt/β-catenin; Apoptosis

Peer-reviewed version available at Cancers 2019, 11, 711; doi:10.3390/cancers11050711

1.Introduction

Prostate cancer (PC) is the third leading cause of cancer death in men in the United States, , with an estimated 164,690 new cases, along with 29,430 deaths, in 2018 [1]. African-American men usually have the greatest susceptibility to developing PC compared to other ethnic groups [2]. The majority of men, during the early stage of the disease, are asymptomatic and develop symptoms only during the advanced stages. The treatment of PC is primarily dependent on the age of the patient, disease stage and aggressiveness of the disease [3]. The majority of the localized disease cases can be cured [4]. However, about 20 to 40% of patients previously designated as being cured of prostate cancer eventually have a recurrence or relapse [5]. Metastatic, aggressive prostate cancer can be treated using androgen deprivation therapy, which is a combination of chemotherapy, hormone therapy and radiotherapy, but this does not produce complete remission [6]. Eventually, PC can progress to the resistant metastatic stage (i.e. castration resistant prostate cancer, CRPC), where patients become resistant to all androgen deprivation treatments [7]. The current treatment regimens can extend the survival of CRPC patients for only a few months [8]. Accordingly, it is essential to develop new treatment strategies with novel mechanisms of action that will overcome resistant metastatic stages and PC recurrence.

The Wnt/β-catenin signaling is involved in the growth and development of several organs, especially during the embryonic stage [9]. The hyperactivation of this pathway occurs predominantly in colon, ovarian, liver and prostate cancers [10]. In PC, the Wnt signaling pathway is involved in the progression of resistant, metastatic stages such as CRPC [11]. Therefore, targeting the Wnt signaling pathway to treat advanced PC could be a potential novel strategy.

The thienopyrimidines are a versatile group of compounds that contain a biologically active pharmacophore [12]. It has been reported that various thienopyrimidine derivatives have efficacy *in vitro* in certain cancer cell lines [12]. However, there are no previous reports regarding the potential anti-metastatic efficacy of any thieno[2,3-*d*]pyrimidine derivatives and the mechanism of action of these compounds [13]. Previously, we reported the synthesis and evaluation of thirteen thieno[2,3-*d*]pyrimidine derivatives (i.e. thieno [2,3-*d*] pyrimidines) [13]. The thienopyrimidine compounds were screened in several cancer cell lines, including colon cancer (HCT116 and HCT115), ovarian cancer (A2780) and brain cancer (LN-229, GBM-10) cell lines. One of the derivatives, compound RP-010, was efficacious in colon cancer cell lines (HCT116, IC_{50}= 0.6 ± 0.3 μM and HCT115, IC_{50} = 0.7 ± 0.2 μM) [13]. Furthermore, RP-010 significantly inhibited cell proliferation in a concentration- and time - dependent manner. To further determine the pharmacological profile of the RP series, we determined their efficacy in the PC cell lines, PC3 and DU145. In addition, the potential anti-metastatic efficacy of the most promising compound, RP-010, was also determined *in vitro*.

2. Results

2.1. RP-010 has efficacy against PC cell lines

Among the 13 RP compounds evaluated **(Figure 1a),** the compound RP-010 had the greatest efficacy in the PC cell lines, DU-145 (IC_{50} = 0.5 μM) and PC3 (IC_{50} = 0.3 μM), compared to the normal cell lines, CRL1459 (IC_{50} = 73 μM) and CHO (IC_{50} = 14 μM) cells ($p < 0.001$ and $p < 0.01$, respectively, **Figure 1b).** The morphological changes in the PC cells incubated with RP-010 (0.1, 0.3, and 1 μM) compared to the vehicle controls, is shown in **Figure 1c**. The colony formation assay was used to determine the effect of RP-010 on the number and size of the colonies formed by the DU-145 and PC3 PC cells. The colony formation rate of DU-145 cells was significantly decreased by 1 ($p < 0.01$) or 2 μM ($p < 0.01$) of RP-010 compared to cells incubated with vehicle (**Figure 1d).** Furthermore, RP-010 (1 or 2 μM) significantly decreased the size of the colonies formed by DU-145 cells compared to cells incubated with vehicle (**Figure 1d)**. A histogram quantitatively summarizing the results is shown in the supplementary data section **(Figure 1S).** Similarly, the colony formation rate of PC3 PC cells was

Peer-reviewed version available at Cancers 2019, 11, 711; doi:10.3390/cancers11050711

significantly decreased by 1 ($p < 0.01$) or 2 μM ($p < 0.01$) of RP-010 compared cells incubated with vehicle (**Figure 1S).**

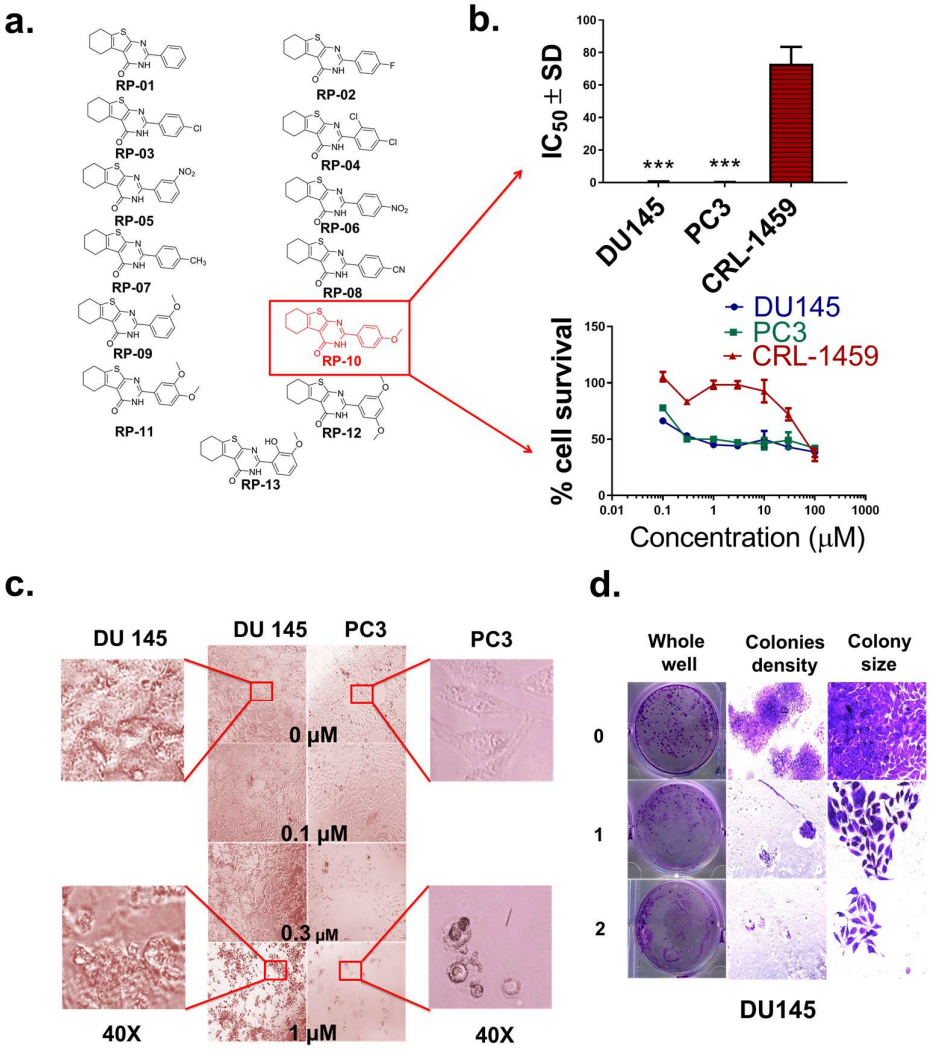

Figure 1. RP-010 cytotoxic effect on prostate cancer cells (a) an illustration of the chemical structures of the thirteen RP compounds evaluated in this study. **(b)** RP-010 cytotoxicity in prostate cancer cells (DU145 and PC3) represented by survival curves and IC_{50} values compared to normal CRL-1459 cells. **(c)** Representative pictures of the morphological changes in cells incubated with RP-010 (0.1, 0.3 or 1 μM) or vehicle for 72 hrs. **(d)** Colony formation assay showing the effect of RP-010 or vehicle (1 or 2 μM) on the colony density (10x) and size (20x) of DU145 cells. All results are presented as the means ± SD of three independent experiments. *$p < 0.05$, **$p < 0.01$, ***$p < 0.001$.

We subsequently determined the efficacy of RP-010 (0.5 or 1 μM) in DU-145 PC cells following incubation for 72 h. DU-145 cells incubated with vehicle continued to grow and divide over time until they reached ≈100% confluence after 72 h (**Figure 2S)**. However, DU-145 cell growth over time was significantly decreased by 0.5 μM of RP-010 ($p < 0.05$) after 24 h of incubation or 1 μM of RP10 ($p < 0.01$) after 12 h of incubation compared to cells incubated with vehicle (Figure 2S).

Table 1: Cytotoxic efficacy data for the RP-010 series (**RP-01 –RP-013**) on prostate cancer cell lines compared to normal cell lines (**IC_{50}** values are shown in μM; NA = not applicable).

RP series	IC_{50}± SD (μM)			
	Prostate		Normal	
	PC3	DU 145	CRL 1459	CHO
RP-01	>100	>100	>100	>100
RP-02	>100	>100	>100	>100
RP-03	>100	>100	>100	>100
RP-04	73.4 ± 3.1	>100	>100	>100
RP-05	>100	>100	>100	>100
RP-06	>100	>100	>100	>100
RP-07	>100	>100	>100	>100
RP-08	6.4 ± 0.5	>100	>100	>100
RP-09	2.8 ± 1.1	>100	>100	>100
RP-010	0.3 ± 0.1	0.5 ± 0.2	73.0 ± 5.3	14.0 ± 1.3
RP-011	6.6 ± 0.7	2.7 ± 0.5	>100	>100
RP-012	6.9 ± 1.0	>100	>100	>100
RP-013	>100	>100	>100	>100

The MTT assay was used to determine cell survival. The IC_{50} values are represented as mean ± SD of three independent experiments. DU145 and PC3 prostate cancer cells were screened, as well as normal epithelial colon (CRL-1459) and normal Chinese hamster ovary cells (CHO).

2.2. RP-010 blocks the PC cell cycle at the G2 phase.

RP-010 significantly altered the distribution of the DU-145 cells in the cell cycle (**Figure 2a).** The DU145 cells were significantly shifted from the G1 phase by 0.5 ($p < 0.05$), 1 ($p < 0.05$) or 2 μM ($p < 0.01$) compared to cells incubated with vehicle (**Figure 2a)**. The DU145 cells significantly accumulated in the G2 phase following incubation with 1 ($p < 0.05$) or 2 μM ($p < 0.05$) compared to cells incubated with vehicle (**Figure 2a)**. Similarly, there was a significant increase in the percentage of PC3 cells in the G2 phase following incubation with 0.5 ($p < 0.01$), 1 ($p < 0.01$) or 2 μM ($p < 0.0001$) compared to cells incubated with vehicle **(Figure 3S).** In contrast to the DU145 cells, there was a significant decrease in the percentage of PC3 cells in the G1 phase following incubation with 0.5 ($p < 0.01$), 1 ($p < 0.01$) or 2 μM ($p < 0.001$, **Figure 3S).** Overall, our results indicated that RP-010 arrested the PC cells at the G2 phase of the cell cycle.

2.3. RP-010 increases oxidative stress in PC cells:

2',7'-dichlorodihydrofluorescein diacetate (H2DCFDA or DCF) was used to determine the effect of RP-010 (0.5, 1, 2 or 4 μM) and vehicle on the generation of oxidative stress in PC cells (DU145 and PC3) after 24 h of incubation. RP-010 resulted in a higher fluorescence of DCF in cells incubated with RP-010 compared to cells incubated with vehicle (**Figure 4S)**. DU145 cells produced significantly higher levels of ROS, following incubation with 0.5 ($p < 0.05$), 1 ($p < 0.01$), 2 ($p < 0.01$) or 4 μM ($p < 0.001$) of RP-010 compared to cells incubated with vehicle (**Figure 4S)**. In PC3 cells, RP-010 also induced higher levels of ROS at different concentrations 1 and 2 ($p < 0.05$), and 4 μM ($p < 0.01$) (**Figure 4S)**.

2.4. RP-010 induces cell death in DU145 and PC3 PC cells by mitotic catastrophe and apoptosis:

The results shown in **Figure 2b and c** indicate that RP-010 induced DU145 and PC3 cell death by two major mechanisms: 1) the formation of giant cells with multi-nuclei (multinucleated giant cells), primarily at the lower concentration and 2) the induction of apoptotic death, predominantly at

Peer-reviewed version available at Cancers 2019, 11, 711; doi:10.3390/cancers11050711

higher concentrations (**Figure 2b and c)**. The incubation of DU145 cells with vehicle produced few or no apoptotic cells (**Figure 2 b and c**). However, the incubation of DU145 cells with 1 μM of RP-010 for 24 h produced multinucleated cells (**Figure 2b)**. However, the incubation of DU145 and PC3 cells with 2 or 4 μM of RP-010 produced a significant increase in the number of highly condensed, fragmented nuclei chromatin, indicative of apoptosis (**Figure 2b**). Similarly, the incubation of DU145 cells with 1, 2 or 4 μM of RP-010 for 48 h primarily produced apoptotic nuclear morphology (**Figure 2c)**. The effect of RP-010 on PC3 cells is shown in **Figure 5S**. The incubation of PC3 cells with 1 μM of RP-010 for 24 and 48 h produced a significant increase in multinuclear morphology and apoptosis at 2 or 4 μM (**Figure 5S**).

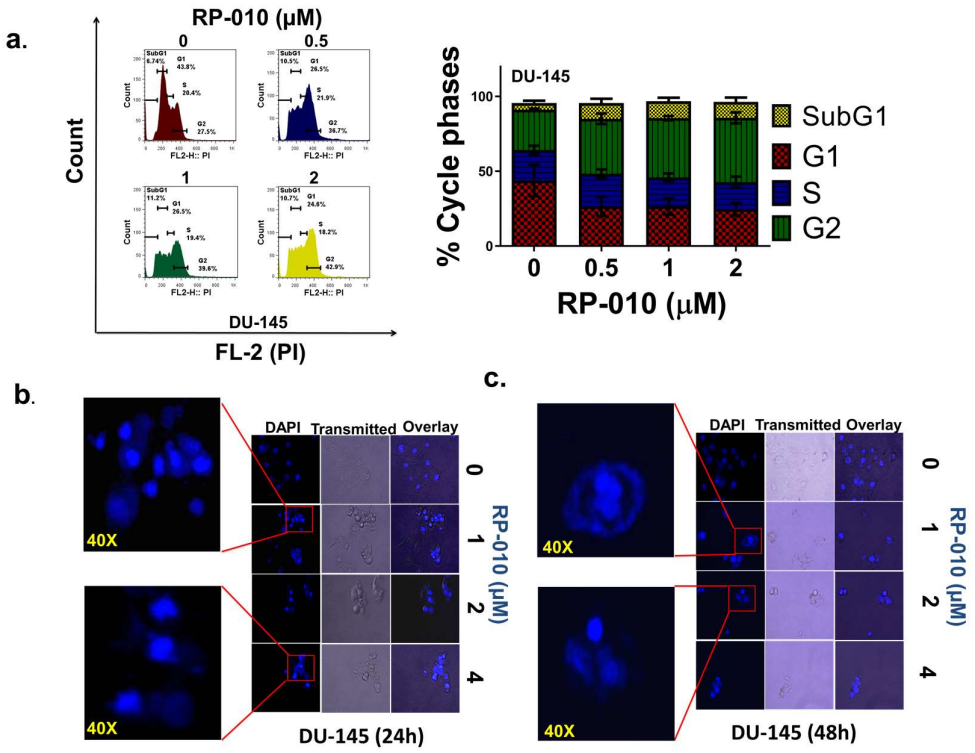

Figure 2. The changes induced by RP-010 on the cell cycle and nuclear events. (a) Analysis of RP-010 (0.5, 1 or 2μM) induced changes on the cell cycle using flow cytometry assay (P1 on the Ordinate and cell count on the abcissa). A graph showing the percent change for each phase following incubation with RP-010 in shown next. In the **(b)** and **(c)** The effects of RP-010 (1, 2 or 4 μM) and vehicle on the nucleus of DU145 cells at 24 and 48h, respectively, are shown. Both chromatin condensation and mitotic catastrophe can be seen.

2.5. RP-010 induces apoptosis by affecting the Bcl-2 family proteins and inducing caspase activation:

We determined the *in vitro* effect of vehicle or 2 μM of RP-010 following 24 h incubation on the expression of the proteins Bak, Bax and Bcl2, caspase 3 and poly ADP-ribose polymerase (PARP), which are involved in the regulation of apoptosis in DU-145 cells. The expression level of Bak in DU145 cells was significantly increased (≥ 2 - fold) following incubation with 1 ($p < 0.01$) or 2 μM ($p < 0.01$) of RP-010 compared to cells incubated with vehicle (**Figure 3**). In contrast, the incubation of DU145 cells with 1 or 2 μM of RP-010 did not significantly alter the expression of the pro-apoptotic protein, Bax (**Figure 3**). The expression level of the anti-apoptotic protein, Bcl2, was significantly decreased by 1 ($p < 0.01$) or 2 μM ($p < 0.01$) of RP-010 compared to cells incubated with vehicle (**Figure 3**).

The generation of cleaved caspase-3, - due to the cleavage of inactive caspase - 3, was significantly increased by incubating DU-145 cells with 1 ($p < 0.001$) or 2 μM ($p < 0.001$) of RP-010 (**Figure 3**). The caspase 3 - mediated cleavage of both cytosolic and nuclear PARP was significantly

Peer-reviewed version available at Cancers 2019, 11, 711; doi:10.3390/cancers11050711

increased in DU-145 cells following incubation with 1 (cytoplasm: $p < 0.05$, nucleus: $p < 0.01$) or 2 μM (cytoplasm: $p < 0.05$, nucleus: $p < 0.01$) of RP-010 compared to cells incubated with vehicle **(Figure 3).** In addition, the levels of cytosolic PARP were significantly reduced by 1 ($p < 0.01$) or 2 μM ($p < 0.001$) compared to cells incubated with vehicle (**Figure 3)**. Furthermore, as expected, the levels of cleaved cytosolic PARP were significantly increased by 1 ($p < 0.05$) or 2 μM of RP10 ($p < 0.05$) compared to cells incubated with vehicle **(Figure 3).** Similarly, the levels of cleaved nuclear PARP were significantly increased following incubation with 1 ($p < 0.01$) or 2 μM ($p < 0.01$) of RP-010 compared to cells incubated with vehicle (**Figure 3**). The incubation of DU-145 cells with 1 or 2 μM of RP-010 did not significantly alter the levels of cytochrome c compared to cells incubated with vehicle **(Figure 3).**

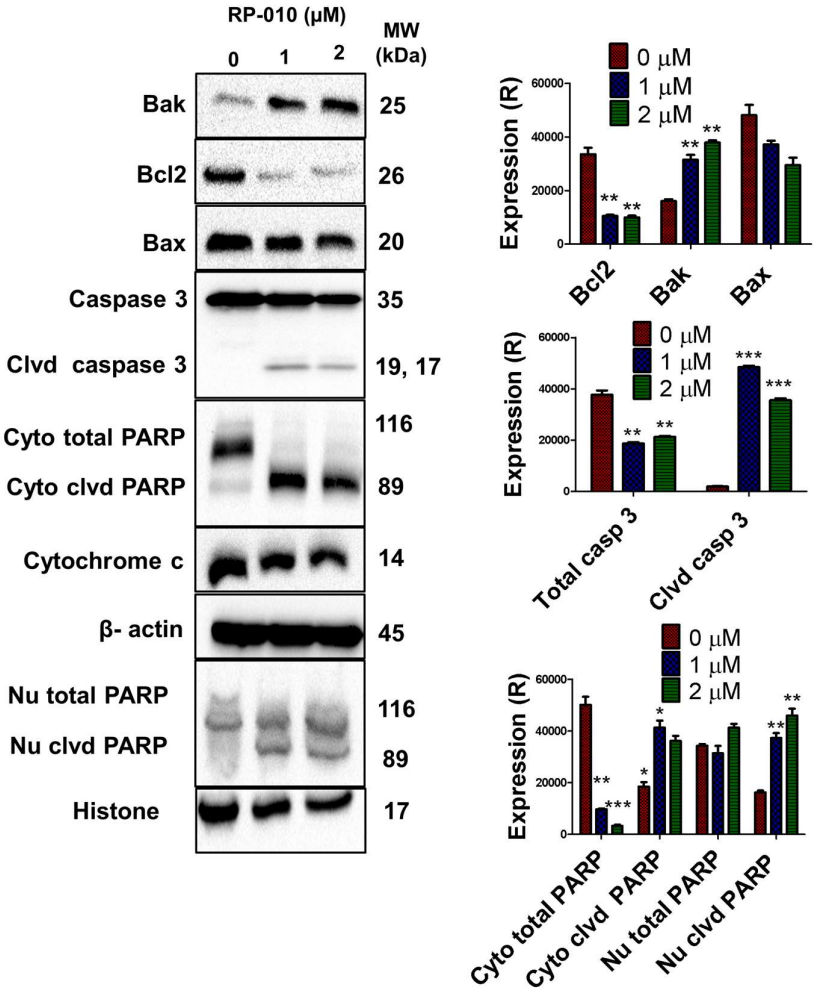

Figure 3. RP-010 activates the intrinsic arm of apoptosis. The effect of RP-010 (1 or 2 μM, at 24 h incubation) or vehicle on the expression levels of the apoptotic proteins Bak, Bcl2, caspase-3, cleaved caspase-3, cytosolic (Cyto) and nuclear (Nu) PARP, cytosolic and nuclear cleaved PARP and cytochrome c are shown. β-actin and histone were used as reference proteins. The histograms represent a quantitative summary of the results. (R) = relative. **$p < 0.01$, ***$p < 0.001$.

2.6. RP-010 inhibits PC cells migration and invasiveness:

It has been reported that DU-145 and PC3 cells can undergo migration and invasiveness and thus, can be used as an *in vitro* model to assess metastasis [14]. Therefore, we used the wound healing and transwell migration assays to determine the effect of RP-010 on DU-145 cell migration and invasiveness. In the wound healing assay, DU-145 cells incubated with RP-010 were

Peer-reviewed version available at Cancers 2019, 11, 711; doi:10.3390/cancers11050711

significantly less likely to migrate compared to cells incubated with vehicle **(Figure 4a).** Indeed, there was a significant decrease in DU-145 cell wound healing following incubation with RP-010. Results were as follows: 1) at 12 h, ($p < 0.001$ for 2 μM only); 2) at 18 h ($p < 0.001$ for all concentrations); 3) at 24 h ($p < 0.001$ for 0.5, 1 and 2 μM, whereas most of the cells were non-viable at 4 μM **Figure 4a**) and 4) at 48 h ($p < 0.001$ for 0.5 and 1 μM. Most of the cells were non-viable after incubation with 2 or 4 μM, **Figure 4a**) compared to cells incubated with vehicle. In contrast, in DU-145 cells incubated with vehicle, there was a rapid closure of the wound area with time and complete closure was detected at 48 h (**Figure 4a)**. In PC3 cells, the effects of RP-010 on wound closure were similar to those for DU-145 cells. The incubation of PC3 cells with RP-010 significantly decreased wound healing and the results were as follows: at 12 h ($p < 0.01$ for 0.5 and $p < 0.001$ for 1, 2, and 4 μM); 2) at 18 h ($p < 0.001$ for all concentrations); 3) at 24 h ($p < 0.001$ for all concentrations) and 4) at 48 h most the cells were dead at concentrations 0.5, 1, or 2 μM, **Figure 6S)**. In contrast, as with DU-145 cells, the induced wound in PC3 cells incubated with vehicle closed completely within 48 h (**Figure 6S).**

In the transwell migration assay, the number of DU-145 cells that migrated across the polycarbonate membranes were significantly decreased following 24 h of incubation with 0.5 ($p < 0.05$) 1 ($p < 0.001$) or 2 μM ($p < 0.001$) of RP-010 compared to cells incubated with vehicle (**Figure 4b**). The migration of PC3 cells was not significantly altered by 0.5 μM (24 h incubation) of RP-010 compared to cells incubated with vehicle (Figure 6S). However, the migration of PC3 cells, compared to cells incubated with vehicle, was significantly decreased by 1 ($p < 0.05$) or 2 ($p < 0.05$) μM of RP-010 (**Figure 6S**).

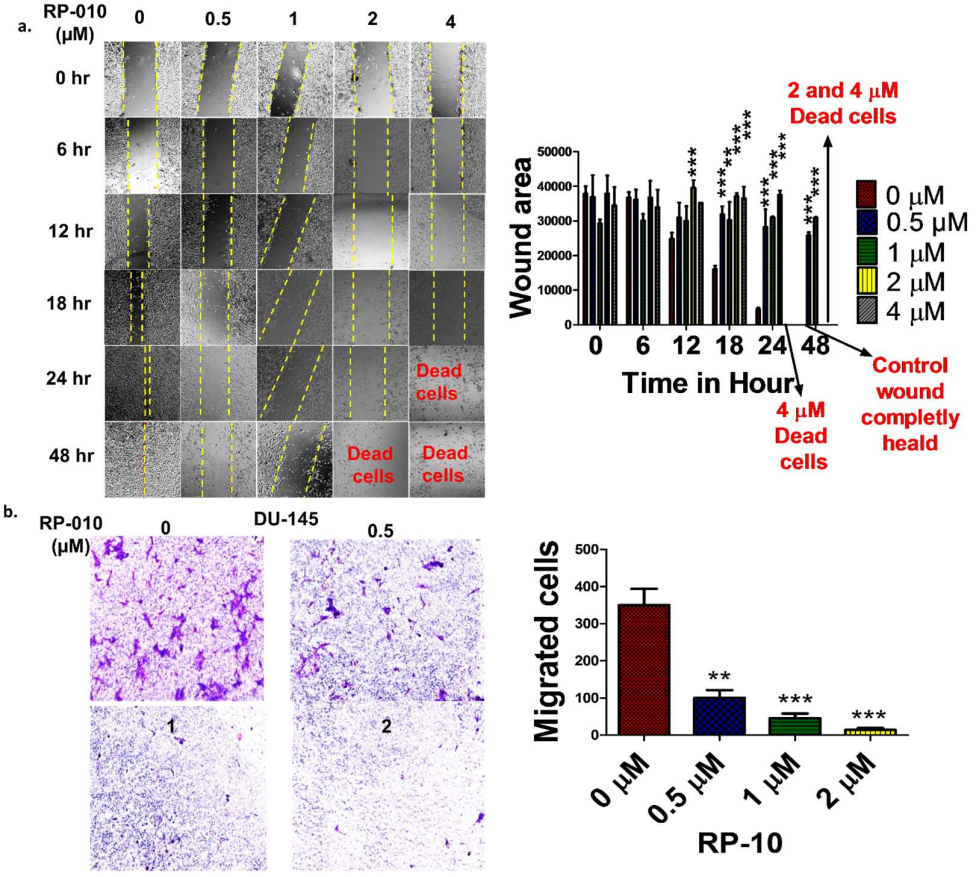

Figure 4. RP-010 significantly reduces cell migration and invasiveness in DU145 cells. (a) The pictures show the results of the wound healing assay following incubation with RP-010 (0.5, 1, 2 or 4 μM) or vehicle and the histogram represents a quantitative summary of the results; **(b)** the pictures

indicate the level of cells that migrated following incubation with RP-010 (0.5, 1 or 2 μM) or vehicle. The histogram represents a summary of the results. **p < 0.01, ***p < 0.001.

2.7. RP-010 downregulates in vitro Wnt/β-catenin signaling in PC cells

We determined the effect of RP-010 (0, 1 or 2 μM, at 24 h incubation) on the expression level of the following nuclear and cytosolic proteins in the **Wnt/β-catenin signaling**: 1) Wnt 5a; 2) DVL3; 3) LRP-6; 4) P-LRP-6; 5) Naked 1; 6) Naked 2; 7) cyclin B1; 8) c- Myc; 9) and 10) β-catenin, in DU-145 PC cells. The levels of DVL3 in DU-145 cells were significantly decreased by 1 ($p < 0.01$) or 2 μM ($p < 0.01$) of RP-010 compared to cells incubated with vehicle **(Figure 5).**

In addition, the level of LRP-6 in DU-145 cells were significantly decreased by 1 ($p < 0.05$) or 2 μM ($p < 0.05$) of RP-010 **(Figure 5).** Similarly, the levels of phosphorylated form of LRP-6, P-LRP-6, were significantly decreased in DU-145cells by 1 or 2 μM of RP-010 ($p < 0.01$ for both concentrations of RP-010) **(Figure 5)**.

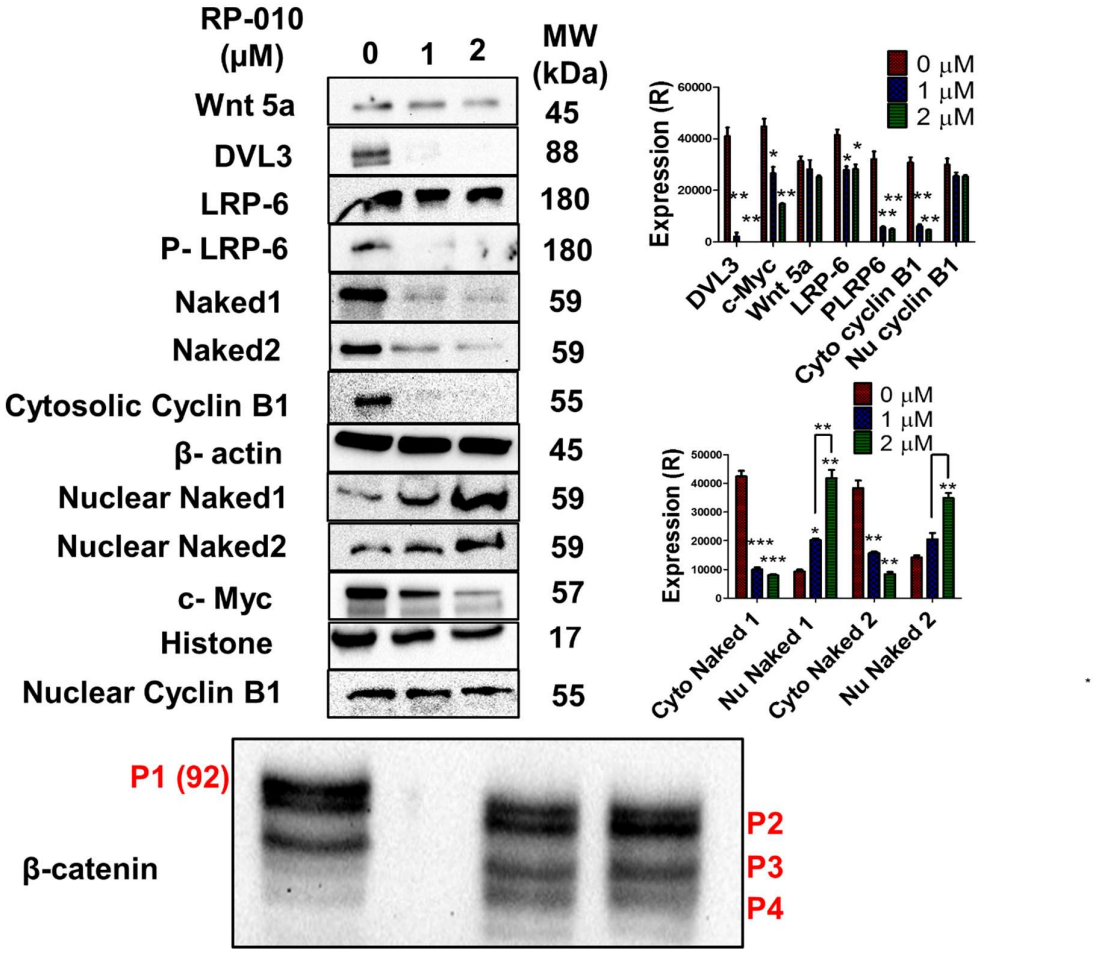

Figure 5. RP-010 induces significant changes in Wnt/ β- catenin signaling. The effect of **RP-010** (1 or 2 μM, at 24 h incubation) or vehicle on the expression level of the following proteins: Wnt 5a, DVL3, LRP-6, P-LRP-6, cytosolic and nuclear Naked1 and 2, cytosolic and nuclear cyclin B, c-Myc and β-catenin. β-actin and histone were used as reference proteins. The histograms represent a quantitively summary of the results. (R) = relative. *p < 0.05, **p < 0.01, ***p < 0.001.

The incubation of DU-145 cells with RP-010 significantly decreased the levels of the cytosolic Naked 1 ($p < 0.001$ for 1 or 2 μM) and Naked 2 proteins ($p < 0.01$ for 1 or 2 μM) compared to cells incubated with vehicle **(Figure 5).** In contrast, the incubation of these cells with RP-010 significantly

increased the nuclear levels of Naked 1($p < 0.05$ for 1 μM and $p < 0.01$ for 2 μM) and Naked 2 compared to cells incubated with vehicle **(Figure 5)**.

The incubation of DU-145 cells with 1 or 2 μM of RP-010 did not significantly alter the levels of E-cadherin compared to cells incubated with vehicle (**Figure 8S**). The cytosolic levels of the protein cyclin B1 were significantly decreased by 1 or 2 μM of RP-010 ($p < 0.01$ for both concentrations), without significantly altering the nuclear levels of this protein, compared to cells incubated with vehicle **(Figure 5)**. The levels of nuclear c-Myc in DU-145 cells was significantly decreased by 1 ($p < 0.05$) or 2 μM ($p < 0.01$) compared to cells incubated with vehicle **(Figure 5)**.

In DU-145 cells, RP-010 (1 and 2 μM) produced a significant fragmentation of the high molecular weight, full - length protein, p92 (or p1), into several lower molecular weight fragments (≈70 kDa) **(Figures 5 and 7S).** There was a significant decrease in the levels of total active β-catenin in DU-145 cells incubated with 1 ($p < 0.01$) or 2 μM ($p < 0.001$) (**Figures 5 and 7S).** This cleavage of total protein produced by RP-010 resulted in the increased accumulation of lower molecular weight fragment, compared to cell incubated with vehicles, that are primarily inactive, including P3 ($p < 0.01$ for 1 or 2 μM), and P4 ($p < 0.05$ for 1 or 2 μM) **(Figure 5 and 7S).** Interestingly, no significant change in the levels of Wnt 5a protein was detected following incubation with RP-010 compared to cells incubated with vehicle (**Figure 5**).

2.8. Effect of RP-010 in an in vivo zebrafish model of toxicity

We used an *in vivo* zebrafish model to assess potential toxic effects of RP-010. The exposure (24 and 48 h) of zebrafish to 0.3, 1, 3, 6, or 10 μM did not significantly increase mortality compared to vehicle **(Figure 6).** None of the concentrations of RP-010 significantly altered the body or tail shapes or their lengths compared to vehicle **(Figure 6a and b).** Furthermore, no malformations were detected following exposure to RP-010 **(Figure 6a and b**). However, at 10 μM, RP-010 produced significant pericardial edema ($p < 0.05$) after 24 or 48 h of exposure (**Figure 6a and b**) compared to exposure to the vehicle. Furthermore, the zebrafish developed a significant loss in dorsoventral balance following 24 or 48 h of exposure to 10 μM of RP-010 compared to vehicle **(Figure 6a and b)**. A significant increase in pericardial edema and irregularities in heart rate were observed ($p < 0.05$) following 24 or 48 h of exposure to 10 μM of RP-010 compared to vehicle **(Figure 6a and b).** The effect of RP-010 on zebrafish heart rate is shown in **Figure 9S.** Overall, our results indicated that RP-010 was well tolerated by zebrafish at concentrations up to 6 μM.

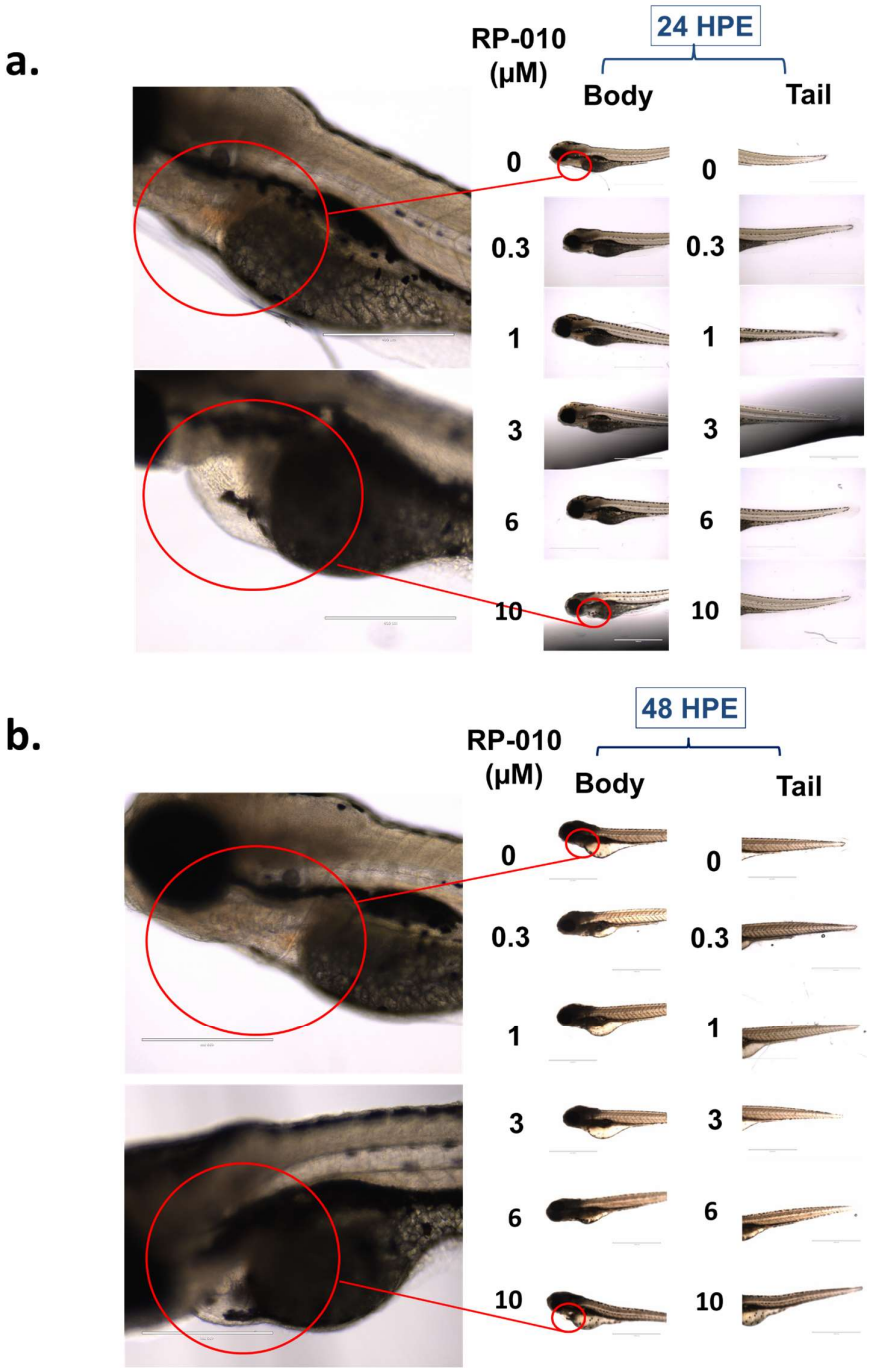

Figure 6. RP-010 toxicity in an *in vivo* zebrafish model. The effect of RP-010 (0.3, 1, 3, 6 or 10 μM) or vehicle treatment on the body and tail of zebrafish after exposure to the above concentrations of RP-010 for 24 or 48 hrs.

3. Discussion

In this study, we conducted experiments to ascertain the efficacy and mechanism of action of the novel thienopyrimidine derivative, RP-010, in PC cells. The thieno[2,3-*d*]pyrimidines were synthesized to structurally resemble natural purines, and the synthetic 4-anilinoquinazoline core in the FDA approved anticancer drugs, gefitinib and erlotinib [15]. and tandutinib [16]. The *in vitro* anticancer efficacy of these thienopyrimidine derivatives have been previously reported [17]. The IC_{50} values in hepatocellular carcinoma cells (HEPG2) for the thienopyrimidine and

triazolothienopyrimidine derivatives were 2-3 μM [17]. In the breast cancer line, MCF-7, the IC_{50} was ≈ 4 μM for the thienopyrimidines derivatives, whereas the IC_{50} was 15 μM for the triazolothienopyrimidine derivatives [18]. Furthermore, thieno[2,3-d] pyrimidine derivatives containing a thiosemicarbazide moiety (compounds 5a-d) had IC_{50} values from 5.3-138 μM in PC3 cells [19]. In contrast, our synthesized thieno[2,3-*d*]pyrimidines compounds had anticancer efficacy in PC3 and DU-145 PC cells, and the compound RP-010 had the highest potency of all of the 13 derivatives (IC_{50} < 1 μM). Previously, it has been reported that the anticancer efficacy of the thienopyrimidine compounds may be due to inhibition of cyclin kinase, inhibition of thymidylate synthase and antagonism of gonadotropin releasing hormone (GnRH) receptor [18,20,21]. The overexpression of the epidermal growth factor receptor (EGFR) and v-erb-b2 erythroblastic leukemia viral oncogene homolog 2 (ErbB2) have been reported to be involved in cancer progression and development, including prostate cancer [22] . The thieno [3, 2-d] pyrimidine (core A) and thieno [2, 3-d] pyrimidine (core B) cores were synthesized and compounds that were derivatives of core A inhibited EGFR and ErbB2, with IC_{50} values of 1-68 nM and 30-705 nM, respectively [23].

The incubation of DU-145 and PC3 PC cells with RP-010 (1, 2 or 4 μM) induced the formation of single cells with multiple nuclei, especially at low concentrations. This morphological change in different cancer cells has been previously reported [24]. This phenomenon has been designated "mitotic catastrophe" or polyploidy and it is a unique mechanism of death that occurs during mitosis [25]. Cells that undergo mitotic catastrophe typically have a reduced proliferative capacity and become flattened and enlarged [26]. Similarly, the compound reversine is efficacious in certain cancers [27]. It induces the formation of multinucleated, giant cells in human prostate, breast and lung cancer cell lines [28,29]. Interestingly, doxorubicin, an FDA approved anticancer drug, induces cell death by apoptosis at high concentrations and mitotic catastrophe at lower concentrations (50 ng/ml) in Huh-7 cells [30]. The cells exit mitosis without cell division, forming a single giant cell with multi-nuclei and decondensed chromatin [27]. Moscatilin also produces the aforementioned changes *in vitro* [31]. This type of cell death could result from the alteration in the regulators of mitosis, including cell-cycle-specific kinases (e.g. cyclin B1-dependent kinase Cdk1, polo-like kinases and aurora kinases), survivin, p53, caspases and proteins in the Bcl-2 family [28]. Currently, the effect of RP-010 on these proteins remains to be elucidated. Bcl2 proteins are important regulators of the intrinsic pathway of apoptosis [32,33]. The activation of the intrinsic apoptotic pathway results in the activation of caspases, cleaving many cellular proteins, including PARP [34]. In addition to multinuclear formation, RP-010 induced apoptotic chromatin condensation in both PC cell lines, particularly at higher concentrations. The canonical Wnt/β-catenin signaling pathway is part of the Wnt signaling pathway [35]. Following the binding of the Wnt protein to its membrane receptors (Frizzled) and the low-density lipoprotein receptor-related protein 6 co-receptors (LRP-6), dishevelled (Dvl) and axin are recruited, resulting in inhibition of β-catenin phosphorylation and degradation [36]. Subsequently, β-catenin is activated and translocated to the nucleus [37]. In the nucleus, β-catenin interacts with specific transcriptional factors (T-cell factor TCF) and lymphoid enhancer factor (LEF), inducing the expression of Wnt responsive proteins such as c-Myc, MMP-7, cyclins, as well as other proteins [38]. The over-activation and accumulation of β-catenin in the nucleus produces progression of colon, ovarian, liver and prostate cancers, among others [9,39,40]. Wnt/β-catenin signaling plays a critical role in cancer cell metastasis and invasiveness [41]. In prostate cancer, β-catenin produces progression and growth in a transgenic mouse model, even in the absence of Wnt signaling [42]. β-catenin can produce highly invasive prostate cancer in several transgenic mouse models (e.g. with SV40 large T-antigen, loss of PTEN, mutated K-ras) [41]. Furthermore, β-catenin nuclear localization was detected in 24% of metastatic samples from patients with metastatic resistant prostate cancer [43]. β-catenin expression is significantly increased in 38% of patients with CRPC compared to 23% of patients with localized, non-metastatic prostate cancer [44]. In 11 of 27 CRPC patients with bone metastasis, the nuclear localization of β-catenin was detected [45]. Therefore, the inhibition of this pathway or the key regulator proteins of this pathway, may represent a novel mechanism to inhibit prostate cancer progression and reverse metastatic

resistant stage as in CRPC. β-catenin has been reported to be degraded in HeLa cells [46]. This results in multiple lower molecular weight products, that typically have weak or no transcriptional efficacy[47]. Previously, we have reported the fragmentation of β-catenin in HCT116 colon cancer cells following incubation with the novel silybin derivative, 15k [48,49]. In this study, the incubation of prostate cancer cells with RP-010 induced the degradation of nuclear β-catenin into smaller fragments, primarily with different or lower transcriptional activity, in prostate cancer cells. The RP-010-indcued fragmentation of β-catenin is a major cellular event that is partially responsible for the anti-proliferative and anti-metastatic efficacy of RP-010.

Additional proteins in the Wnt/β-catenin signaling pathway have essential roles in the activation of this pathway. For example, LRP-6 receptors are needed to signal the early events produced by Wnt binding in the cytosol [36] .The intracellular domain of LRP6 is phosphorylated at specific serine and threonine residues by GSK3 and casein kinase (CK) upon activation of Wnt signaling [50]. The protein CD44 activates LRP-6 phosphorylation, inducing an upregulation of the proteins in the Wnt signaling pathway [51]. The inhibition of LRP-6 phosphorylation downregulates Wnt/β-catenin signaling. For example, triptolide, a diterpene epoxide derived from a natural product, inhibits LRP-6 phosphorylation and pancreatic cancer proliferation in a mouse model (KPC ($Kras^{G12D}$, $P53^{R172H}PDX^{Cre}$) of pancreatic-derived tumors [52]. In this study, RP-010 significantly downregulated LRP-6 expression. RP-010 produced a significantly greater inhibition the phosphorylation of LRP-6 than downregulating the total protein, thereby contributing to its multi-target mechanism of action. Disheveled protein 3 (DVL3) also plays a role in β-catenin activation and stabilization, where it prevents GSK3B - induced phosphorylation of β-catenin [36]. The increased expression of DVL3 was recently investigated as a biomarker for the recurrence of PC [53]. Furthermore, the inhibition of DVL3 expression and activity enhanced the sensitivity of prostate and breast cancer cells to insulin-like growth factor 1 (IGF1) [54]. Therefore, the inhibition of this protein can result in a reduction in β-catenin activation and its subsequent nuclear translocation [55]. RP-010, *in vitro*, induced a significant downregulation in the cytosolic levels of this protein, thus promoting further inhibition in the Wnt/β-catenin signaling pathway.

The proteins Naked cuticle homologs 1 and 2 (Naked 1 and Naked 2) are important down regulators of the Wnt signaling pathway [35]. The inhibition of the activity of Naked 1 and Naked 2 induces Wnt signaling over-activation and subsequent cancer cell growth and proliferation [56]. The epigenetic silencing of Naked 2 by methylation of the promoter region induced breast cancer growth and proliferation in 7 prostate cancer cell lines [57]. Naked 2 reverses the effects of Wnt/β-catenin in both zebrafish and HEK293 cells [58]. Naked 1 forms a Tcf/β-catenin/Naked1 heterotrimeric complex and is a negative regulator of this pathway in human colorectal cancer cells [35]. Naked 1 binds to β-catenin and inhibits its nuclear translocation in zebrafish embryos [59]. The silencing of the methylation of the promoter Naked 2 produces gastric cancer proliferation, metastasis and migration both *in vitro* (gastric cell lines) and *in vivo* (gastric xenograft mouse model). However, the restoration of Naked 2 efficacy and expression inhibited cancer growth, induced G2/M cycle arrest, inhibited cell migration and restored the anticancer efficacy of docetaxel [60]. RP-010 (1 or 2 μM) significantly induced the translocation of Naked 1 and Naked 2 proteins from the cytosol to the nucleus, as there was a significant decrease in Naked 1 and 2 levels in the cytosol. This *in vitro* finding is novel and may, in part, contribute to RP-010's anticancer efficacy. Further experiments will be required to delineate the effects of RP-010 on the nuclear functions and transcriptional activities of Naked 1 and Naked 2.

The cell cycle regulatory protein, cyclin B1, plays a significant role in cancer development, progression and metastasis [61,62]. The inhibition of cyclin B1 induced G2 cell cycle arrest and apoptosis in PC cells following imiquimod treatment both *in vitro* and *in vivo* [63]. In contrast, the upregulation of cyclin B1 reverses metastasis in colorectal cancer cells [64]. Several anticancer drugs such as flavopiridol, palbociclib, significantly inhibit the expression and activity of cellular cyclins,

Peer-reviewed version available at Cancers 2019, 11, 711; doi:10.3390/cancers11050711

such as cyclin B1 [65]. Currently, the exact role of cyclin B1 in cancer cell growth remains to be determined. RP-010 (1 or 2 μM) significantly decreased the expression levels of cytosolic cyclin B levels without significantly altering its nuclear levels. The RP-010-induced decrease in cyclin B1 levels sensitizes DU145 PC cells and inhibits its proliferation. The myc gene (c-Myc) codes for the protein, c-Myc, which induces significant changes in Wnt signaling by inhibiting GSK3β activity, which phosphorylates and inactivates β-catenin [66]. The c-Myc protein is upregulated by the nuclear translocation of β-catenin [67]. RP-010 (1 or 2 μM) significantly decreased the expression levels of c-Myc to a greater magnitude in DU145 compared to PC3 cells.

Epithelial mesenchymal transition (EMT) is involved in the development, progression, metastasis, and resistance of cancer [68]. Cancer cells with the EMT phenotype can migrate from the extracellular matrix and reach distant tissues [69]. The loss of E-cadherin protein and upregulation of N-cadherin are important markers for the mesenchymal shift [70,71]. The Wnt/β-catenin-signaling cascade is predominantly involved in EMT progression[72]. RP-010 (1 and 2 μM) did not significantly alter the expression levels of either E-cadherin or N-cadherin. These results suggest that RP-010 does not significantly affect two major proteins in the EMT pathway and that the anticancer efficacy of RP-010 may occur via mainly through the induction of apoptosis and inhibition of Wnt/β-catenin signaling.

4. Materials and Methods

4.1. Reagents:

The primary and secondary antibodies were purchased from Cell Signaling Technology (Danvers, MA, USA). Propidium iodide (PI) dye was purchased from Life Technologies (Eugene, Oregon, USA). Dulbecco's modified Eagle's medium (DMEM) was purchased from GE Healthcare Life Sciences, HyClone Laboratories (Logan, Utah, USA). The 0.25% trypsin + 2.2 mM ethylenediaminetraacetic acid (EDTA) and phosphate buffer saline (PBS) were purchased from Mediatech, Inc. (Corning subsidiaries, Manassas, VA, USA). Crystal violet dye powder was purchased from Sigma-Aldrich (St. Louis, MO 63103 USA). Corning® transwell inserts (24 mm Transwell with 8.0 μm pore polycarbonate membrane insert, TC-treated, w/lid, sterile, 24/cs) were purchased from Sigma-Aldrich (St. Louis, MO 63103 USA). The compound 3-(4,5dimethylthiazol-2-yl)-2,5-diphenyltetrazolium bromide (MTT) was purchased from Calbiochem EMD Millipore (Billerica, MA, USA). Clarity™ and Clarity Max™ Western ECL blotting substrates were purchased from Bio-Rad Laboratories (Hercules, CA, USA).

4.2. Cell lines and culture:

The PC cell lines, DU-145 and PC3, as well as normal cell lines (CRL-1459 and CHO) were a kind gift from late Dr. Gary Kruh. All the cells were cultured as adherent monolayers in culturing flasks and were used to determine the anti-cancer efficacy of RP-010. DMEM supplemented with 4.5 g of glucose, 10% fetal bovine serum (FBS) and 1% penicillin/streptomycin, was used to augment cell growth. Finally, the cells were incubated and grown in a humidified incubator containing 5% CO_2 at 37°C [73]. All of cells were checked and confirmed to be free of fungi and mycoplasma. Cells were obtained from frozen stocks and cell passaging (up to P4) was performed at 80% cell confluency by PBS and trypsin + 2.2mM EDTA.

4.3. Cell cytotoxicity Assays:

4.3.1. MTT assay:

The 3-(4,5-dimethylthiazol-2-yl)-2,5-diphenyltetrazolium bromide (MTT) assay was used to determine the cytotoxic efficacy of the RP compounds in the PC cell lines as previously described [74,75]. The RP compounds (1-13) were evaluated in each cell line at serial dilutions ranging

Peer-reviewed version available at Cancers 2019, 11, 711; doi:10.3390/cancers11050711

from1-100 μM. A comparison was made between the cytotoxicity of RP-010 in the PC cells and normal cells (Chinese hamster ovarian: CHO, normal epithelial colon: CRL1459).

4.3.2. Colony formation assay:

This assay was performed as previously described [49]. The DU-145 and PC3 PC cells were incubated with RP-010 (1 or 2 μM) for 24 h. The colonies were fixed and incubated with 0.1% crystal violet dye for 30 mins. After 12 h of incubation, the medium was discarded and cells were trypsinized one time with 0.25% trypsin, 2.21mM EDTA, harvested, counted and reseeded in 6 well plates at a low density (500 cell/well). The cells were allowed to form colonies for 10–14 days at 37◦C, with the medium being changed every other day. Subsequently, methanol was used to fix the colonies formed in each plate, followed by dyeing the colonies with 0.1% crystal violet dye for 30min. Finally, colonies were viewed and counted under an EVOS microscope (Themo Fisher Scientific, Wayne, MI, USA). The colony formation rate equation was applied for each compound: Colony formation rate = number of colonies/number of seeded cells × 100 %.

4.3.3. Time - dependent studies with RP-010:

The cytotoxicity of RP-010 over time was determined using DU-145 PC cells. The cells were seeded and incubated as previously described [48]. The DU-145 cells were incubated with vehicle or RP-010 for 72 h. The pictures were taken over time, at a snapshot interval of 15 min from the same spot of the flask using the CytoSMART™ Lux 10X system (LONZA biosciences (Walkersville, MD, USA) for live cell imaging.

4.4. Cell cycle analysis:

The effect of RP-010 on the cell cycle phases and function was determined using cell cycle analysis with PI staining, followed by flow cytometry [74,76]. The cells were incubated with either vehicle or RP-010 (0.5, 1 or 2 μM) for 24 h. After incubation overnight, the cells were collected, washed and resuspended as an ice-cold PBS suspension. The DNA was stained with PI for at least 15 min on ice. A FACS Calibur flow cytometer from BD Biosciences (San Jose, CA) was used to detect the distribution of the cells following incubation with vehicle or RP-010. Finally, the data were viewed and analysed by FlowJo v10.2 software from FlowJo LLC (Ashland, OR).

4.5. Detection of oxidative stress in PC cells:

The compound 2',7'-dichlorofluorescin (H2DCFDA) was used to detect changes in the oxidative stress status, as previously described [13,49]. in PC3 and DU145. After 24 h of incubation with 0, 0.5, 1, and 4 μM of RP-010, the cells were incubated with H2DCFDA for 30 minutes at 37 °C. The cells were then washed 3 times with 1X PBS for 5 minutes each. The level of reactive oxygen species was then measured based on the fluorescence level of oxidized H2DCFDA dye (excitation at 485nm and emission at 535) using EVOS digital fluorescent microscope 40x.

4.6. DAPI staining:

The nuclear changes in DU-145 and PC3 cells lines produced by incubation for 24 and 48 h with RP-010 (1, 2 and 4 μM) were determined. The cells were seeded on culture cover glass added on 6 well plates and allowed to grow overnight. The cells were then incubated with RP-010 for an additional 24 h at 37°C. The incubated cells were fixed with 4% paraformaldehyde, followed by permeabilization with 0.3% of Triton X100 in PBS for 25 min. Finally, DAPI staining was added and cells were pictured using EVOS microscope.

4.7. Migration and invasiveness assays

4.7.1. Wound healing assay:

This assay was conducted using DU-145 and PC3 cells as previously described [48,49]. Upon confluence, 200 µl sterile tips were used to create a wound by gentle scratching of the complete cell monolayer. Sterile PBS was used to wash the cells several times to remove any floating cells. Different concentrations of the test compound were prepared in the culture media and added immediately after wound formation. The closure of the wound was observed by taking pictures at different time points by an EVOS microscope. Finally, the area of the wounds at different time points was calculated using Image J software (NIH, Bethesda, Maryland, USA).

4.7.2. Transwell migration assay:

The assay was done as previously described [49]. The effect of RP-010, (0.5, 1 or 2 µM) on the invasiveness of PC cells was tested using 24 trans-well inserts with an 8 µM pore size. The addition of the insert to the well forms two chambers (upper and lower), where the upper chamber was used to grow the cells on the porous membrane. The lower chamber was filled with 600 µl of cell-free DMEM medium. A 200 µl of cell suspension was added to each insert and allowed to attach for 1 h. The test compound was added in different concentrations and incubated with the cells for 24 h. Cells that did not migrate were removed from the upper chamber by a cotton swab. Finally, the remaining migrated cells were fixed by methanol and dyed with 0.1% crystal violet dye and observed with an EVOS microscope. The number of migrated cells was counted and compared between the treated and control cells.

4.8. Subcellular fractionation and Western analysis:

DU-145 cells were incubated with RP-010 ((1 or 2 µM) for 24 h. Thereafter, the cells were subjected to a two-step lysis process to extract and separate the cytosolic and the nuclear proteins as previously described [49]. Next, protein separation for both cytosolic and nuclear proteins was achieved by loading the samples in an acrylamide SDS-PAGE. Then, a PVDF membrane was used to transfer the separated proteins. The PVDF membrane was then incubated over night with the following primary antibodies: rabbit α-tubulin, 1:4000 dilution, rabbit BAX (1:1000), rabbit BAK (1:1000), rabbit cytochrome c (1:1000), rabbit PARP (1:5000), rabbit β-Catenin (1:4000), rabbit DVL3 (1:4000), rabbit LRP-6 (1:1000), rabbit P-LRP-6 (1:1000), rabbit c-Myc (1: 4000), rabbit cyclin B1 (1:2000), rabbit Wnt 5a (1:1000), rabbit naked 1 and naked 2 (1:1000), mouse E-cadherin (1:4000), mouse N-cadherin (1;4000), mouse β-actin (1:5000) and rabbit histone (1:3000). Finally, protein expression levels were determined as described previously [77]. All the protein blots above β-actin are cytosolic lysates. All the proteins below β-actin and above Histone (loading control) are nuclear lysates.

4.9. Evaluation of RP-010 toxicity in zebrafish in vivo:

The zebrafish toxicity studies were conducted as previously described [48]. The 5 day-post fertilization larvae (5 fish/well) were exposed to vehicle or RP-010 (0.3, 1, 3, 6, and 10 µM). Subsequently, the zebrafish were observed visually, and pictures were taken at 24 and 48 h post exposure (hpe). The zebrafish were observed for death, changes in swim position, cardiac toxicities (i.e. changes in heart rate and cardiac swelling or edema), and any morphological changes and malformations in the body and tail. The zebrafish studies were approved by the University of Toledo Institutional Animal Care and Use Committee (#105414, approved on 10/2018).

4.8. Statistical analysis:

The data from the wound healing assay, cell cycle assay, MitoTracker Red and Alexa Fluor 488 annexin V assay were analyzed using a two-way analysis of variance (ANOVA), and post-hoc

Peer-reviewed version available at Cancers 2019, 11, 711; doi:10.3390/cancers11050711

analysis was done using Bonferroni's multiple comparison test. The data from the colony formation assay, Western blots, transwell migration assay and Hoechst staining were analyzed using a one-way ANOVA, and post hoc analysis was done using Tukey's multiple comparison test. All of the experiments were repeated in triplicate. The results were expressed as the mean ± the standard deviation (SD). The *a priori* significance level was $p < 0.05$.

5. Conclusion

RP-010 induced the death of DU-145 and PC3 cells via mitotic catastrophe and induction of apoptosis. RP-010 induced apoptosis by 1) upregulating Bak levels 2) downregulating Bcl2 expression levels and 3) cleaving inactive caspase 3 to produce active caspase 3. RP-010 inhibited the Wnt/β-catenin signaling pathway by inducing β-catenin fragmentation, downregulating important proteins in the pathway, i.e. LRP-6, DVL3, and c- Myc. Finally, RP-010 reversed the migration and invasiveness of prostate cells in a time- and concentration - dependent manner. RP-010 may be a promising anticancer compound for metastatic prostate cancer and it did not produce overt toxicity in an *in vivo* zebrafish model. Future mechanistic and *in vivo* efficacy studies are needed to optimize the lead compound RP-010 for clinical use.

Author Contributions Conceptualization, A.K.T., P.T., S.H.S.B., H.A.; Methodology, A.K.T., H.A., C.K. N.H.; Validation, N.H., D.R.; Formal Analysis, A.K.T., C.R.A., F.E.W., H.A.; Resources, A.K.T., S.H.S.B., P.T.; Writing – Reviewing and Editing, H.A., A.K.T., C.R.A.; Project administration and Supervision, A.K.T.; Funding Acquisition, A.K.T.

Funding: This research was funded by the University of Toledo start-up (F110760) to A.K.T.

Acknowledgments: We would like to thank Charisse Montgomery, University of Toledo for editorial assistance. The authors acknowledge Schrödinger, Inc., New York for providing a demo version of the Schrödinger Small Molecule Drug Discovery Suite Ver. 2018-1 for this study.

Conflicts of Interest: The authors declare no conflicts of interest.

References

1. Siegel, R.; Miller, K.; Jemal, A. Cancer statistics (2018) CA Cancer J Clin 2018 68 (1): 7–30. DOI.
2. Selley, S.; Donovan, J.; Faulkner, A.; Coast, J.; Gillatt, D. Diagnosis, management and screening of early localised prostate cancer. **1997**.
3. Litwin, M.S.; Tan, H.-J. The diagnosis and treatment of prostate cancer: a review. *Jama* **2017**, *317*, 2532-2542.
4. Cooperberg, M.R.; Carroll, P.R. Trends in management for patients with localized prostate cancer, 1990-2013. *Jama* **2015**, *314*, 80-82.
5. Ahlering, T.; Skarecky, D. Long-term outcome of detectable PSA levels after radical prostatectomy. *Prostate cancer and prostatic diseases* **2005**, *8*, 163.
6. Miller, K.D.; Siegel, R.L.; Lin, C.C.; Mariotto, A.B.; Kramer, J.L.; Rowland, J.H.; Stein, K.D.; Alteri, R.; Jemal, A. Cancer treatment and survivorship statistics, 2016. *CA: a cancer journal for clinicians* **2016**, *66*, 271-289.
7. Ceder, J.; Elgqvist, J. Targeting prostate cancer stem cells with alpha-particle therapy. *Frontiers in oncology* **2017**, *6*, 273.
8. Scher, H.I.; Fizazi, K.; Saad, F.; Taplin, M.-E.; Sternberg, C.N.; Miller, K.; de Wit, R.; Mulders, P.; Chi, K.N.; Shore, N.D. Increased survival with enzalutamide in prostate cancer after chemotherapy. *New England Journal of Medicine* **2012**, *367*, 1187-1197.
9. Polakis, P. Wnt signaling in cancer. *Cold Spring Harbor perspectives in biology* **2012**, *4*, a008052.

10. White, B.D.; Chien, A.J.; Dawson, D.W. Dysregulation of Wnt/β-catenin signaling in gastrointestinal cancers. *Gastroenterology* **2012**, *142*, 219-232.
11. Yokoyama, N.N.; Shao, S.; Hoang, B.H.; Mercola, D.; Zi, X. Wnt signaling in castration-resistant prostate cancer: implications for therapy. *American journal of clinical and experimental urology* **2014**, *2*, 27.
12. Ghith, A.; Ismail, N.S.; Youssef, K.; Abouzid, K.A. Medicinal Attributes of Thienopyrimidine Based Scaffold Targeting Tyrosine Kinases and Their Potential Anticancer Activities. *Archiv der Pharmazie* **2017**, *350*, 1700242.
13. Amawi, H.; Karthikeyan, C.; Pathak, R.; Hussein, N.; Christman, R.; Robey, R.; Ashby Jr, C.R.; Trivedi, P.; Malhotra, A.; Tiwari, A.K. Thienopyrimidine derivatives exert their anticancer efficacy via apoptosis induction, oxidative stress and mitotic catastrophe. *European journal of medicinal chemistry* **2017**, *138*, 1053-1065.
14. Xia, Q.; Li, C.; Bian, P.; Wang, J.; Dong, S. Targeting SMAD3 for inhibiting prostate cancer metastasis. *Tumour Biol* **2014**, *35*, 8537-8541, doi:10.1007/s13277-014-2368-0.
15. Wakeling, A.E.; Guy, S.P.; Woodburn, J.R.; Ashton, S.E.; Curry, B.J.; Barker, A.J.; Gibson, K.H. ZD1839 (Iressa): an orally active inhibitor of epidermal growth factor signaling with potential for cancer therapy. *Cancer research* **2002**, *62*, 5749-5754.
16. DeAngelo, D.J.; Stone, R.M.; Heaney, M.L.; Nimer, S.D.; Paquette, R.L.; Klisovic, R.B.; Caligiuri, M.A.; Cooper, M.R.; Lecerf, J.-M.; Karol, M.D. Phase 1 clinical results with tandutinib (MLN518), a novel FLT3 antagonist, in patients with acute myelogenous leukemia or high-risk myelodysplastic syndrome: safety, pharmacokinetics, and pharmacodynamics. *Blood* **2006**, *108*, 3674-3681.
17. Gangjee, A.; Qiu, Y.; Kisliuk, R.L. Synthesis of classical and nonclassical 2‐amino‐4‐oxo‐6‐benzylthieno‐[2, 3‐d] pyrimidines as potential thymidylate synthase inhibitors. *Journal of heterocyclic chemistry* **2004**, *41*, 941-946.
18. Shaaban, M.A.; Ghorab, M.M.; Heiba, H.I.; Kamel, M.M.; Zaher, N.H.; Mostafa, M.I. Novel Thiophenes, Thienopyrimidines, and Triazolothienopyrimidines for the Evaluation of Anticancer and Augmentation Effects of γ‐Radiation. *Archiv der Pharmazie* **2010**, *343*, 404-410.
19. Salib, S.B.; Khalil, O.M.; Kamel, M.M.; El-Dash, Y. Synthesis and antitumor activity of novel thienopyrimidine derivatives containing thiosemicarbazide moiety. *Open Access Library Journal* **2016**, *3*, 1.
20. Fujino, M.; Fukuda, T.; Shinagawa, S.; Kobayashi, S.; Yamazaki, I.; Nakayama, R.; Seely, J.; White, W.; Rippel, R. Synthetic analogs of luteinizing hormone releasing hormone (LH-RH) substituted in position 6 and 10. *Biochemical and biophysical research communications* **1974**, *60*, 406-413.
21. Guo, Z.; Chen, Y.; Wu, D.; Zhu, Y.-F.; Struthers, R.S.; Saunders, J.; Xie, Q.; Chen, C. Synthesis and structure–Activity relationships of thieno [2, 3-d] pyrimidine-2, 4-dione derivatives as potent GnRH receptor antagonists. *Bioorganic & medicinal chemistry letters* **2003**, *13*, 3617-3622.
22. Johnston, J.B.; Navaratnam, S.; Pitz, M.W.; Maniate, J.M.; Wiechec, E.; Baust, H.; Gingerich, J.; Skliris, G.P.; Murphy, L.C.; Los, M. Targeting the EGFR pathway for cancer therapy. *Current medicinal chemistry* **2006**, *13*, 3483-3492.

23. Rheault, T.R.; Caferro, T.R.; Dickerson, S.H.; Donaldson, K.H.; Gaul, M.D.; Goetz, A.S.; Mullin, R.J.; McDonald, O.B.; Petrov, K.G.; Rusnak, D.W. Thienopyrimidine-based dual EGFR/ErbB-2 inhibitors. *Bioorganic & medicinal chemistry letters* **2009**, *19*, 817-820.
24. Andreassen, P.R.; Lacroix, F.B.; Lohez, O.D.; Margolis, R.L. Neither p21WAF1 nor 14-3-3σ prevents G2 progression to mitotic catastrophe in human colon carcinoma cells after DNA damage, but p21WAF1 induces stable G1 arrest in resulting tetraploid cells. *Cancer research* **2001**, *61*, 7660-7668.
25. Castedo, M.; Perfettini, J.-L.; Roumier, T.; Andreau, K.; Medema, R.; Kroemer, G. Cell death by mitotic catastrophe: a molecular definition. *Oncogene* **2004**, *23*, 2825.
26. Dimri, G.P.; Lee, X.; Basile, G.; Acosta, M.; Scott, G.; Roskelley, C.; Medrano, E.E.; LINskENs, M.; Rubelj, I.; Pereira-Smith, O. A biomarker that identifies senescent human cells in culture and in aging skin in vivo. *Proceedings of the National Academy of Sciences* **1995**, *92*, 9363-9367.
27. D'Alise, A.M.; Amabile, G.; Iovino, M.; Di Giorgio, F.P.; Bartiromo, M.; Sessa, F.; Villa, F.; Musacchio, A.; Cortese, R. Reversine, a novel Aurora kinases inhibitor, inhibits colony formation of human acute myeloid leukemia cells. *Molecular cancer therapeutics* **2008**, *7*, 1140-1149.
28. Lu, Y.-C.; Lee, Y.-R.; Liao, J.-D.; Lin, C.-Y.; Chen, Y.-Y.; Chen, P.-T.; Tseng, Y.-S. Reversine induced multinucleated cells, cell apoptosis and autophagy in human non-small cell lung cancer cells. *PloS one* **2016**, *11*, e0158587.
29. Kuo, C.-H.; Lu, Y.-C.; Tseng, Y.-S.; Shi, C.-S.; Chen, S.-H.; Chen, P.-T.; Wu, F.-L.; Chang, Y.-P.; Lee, Y.-R. Reversine induces cell cycle arrest, polyploidy, and apoptosis in human breast cancer cells. *Breast Cancer* **2014**, *21*, 358-369.
30. Eom, Y.-W.; Kim, M.A.; Park, S.S.; Goo, M.J.; Kwon, H.J.; Sohn, S.; Kim, W.-H.; Yoon, G.; Choi, K.S. Two distinct modes of cell death induced by doxorubicin: apoptosis and cell death through mitotic catastrophe accompanied by senescence-like phenotype. *Oncogene* **2005**, *24*, 4765.
31. Chen, C.-A.; Chen, C.-C.; Shen, C.-C.; Chang, H.-H.; Chen, Y.-J. Moscatilin induces apoptosis and mitotic catastrophe in human esophageal cancer cells. *Journal of medicinal food* **2013**, *16*, 869-877.
32. Siddiqui, W.A.; Ahad, A.; Ahsan, H. The mystery of BCL2 family: Bcl-2 proteins and apoptosis: an update. *Archives of toxicology* **2015**, *89*, 289-317.
33. De Bono, J.S.; Logothetis, C.J.; Molina, A.; Fizazi, K.; North, S.; Chu, L.; Chi, K.N.; Jones, R.J.; Goodman Jr, O.B.; Saad, F. Abiraterone and increased survival in metastatic prostate cancer. *New England Journal of Medicine* **2011**, *364*, 1995-2005.
34. Hsieh, T.-C.; Traganos, F.; Darzynkiewicz, Z.; Wu, J.M. The 2, 6-disubstituted purine reversine induces growth arrest and polyploidy in human cancer cells. *International journal of oncology* **2007**, *31*, 1293.
35. Stancikova, J.; Krausova, M.; Kolar, M.; Fafilek, B.; Svec, J.; Sedlacek, R.; Neroldova, M.; Dobes, J.; Horazna, M.; Janeckova, L. NKD1 marks intestinal and liver tumors linked to aberrant Wnt signaling. *Cellular signalling* **2015**, *27*, 245-256.
36. MacDonald, B.T.; Tamai, K.; He, X. Wnt/β-catenin signaling: components, mechanisms, and diseases. *Developmental cell* **2009**, *17*, 9-26.

37. Valenta, T.; Hausmann, G.; Basler, K. The many faces and functions of β - catenin. *The EMBO journal* **2012**, *31*, 2714-2736.
38. Sprowl, S.; Waterman, M.L. Past Visits Present: TCF/LEFs Partner with ATFs for β-Catenin–Independent Activity. *PLoS genetics* **2013**, *9*, e1003745.
39. Chiurillo, M.A. Role of the Wnt/β-catenin pathway in gastric cancer: An in-depth literature review. *World journal of experimental medicine* **2015**, *5*, 84.
40. Chen, Z.; He, X.; Jia, M.; Liu, Y.; Qu, D.; Wu, D.; Wu, P.; Ni, C.; Zhang, Z.; Ye, J. β-catenin overexpression in the nucleus predicts progress disease and unfavourable survival in colorectal cancer: a meta-analysis. *PLoS One* **2013**, *8*, e63854.
41. Francis, J.C.; Thomsen, M.K.; Taketo, M.M.; Swain, A. β-catenin is required for prostate development and cooperates with Pten loss to drive invasive carcinoma. *PLoS genetics* **2013**, *9*, e1003180.
42. Yu, X.; Wang, Y.; Jiang, M.; Bierie, B.; Roy - Burman, P.; Shen, M.M.; Taketo, M.M.; Wills, M.; Matusik, R.J. Activation of β - Catenin in mouse prostate causes HGPIN and continuous prostate growth after castration. *The Prostate* **2009**, *69*, 249-262.
43. Chesire, D.R.; Ewing, C.M.; Gage, W.R.; Isaacs, W.B. In vitro evidence for complex modes of nuclear β-catenin signaling during prostate growth and tumorigenesis. *Oncogene* **2002**, *21*, 2679.
44. de la Taille, A.; Rubin, M.A.; Chen, M.-W.; Vacherot, F.; de Medina, S.G.-D.; Burchardt, M.; Buttyan, R.; Chopin, D. β-Catenin-related anomalies in apoptosis-resistant and hormone-refractory prostate cancer cells. *Clinical Cancer Research* **2003**, *9*, 1801-1807.
45. Wan, X.; Liu, J.; Lu, J.-F.; Tzelepi, V.; Yang, J.; Starbuck, M.W.; Diao, L.; Wang, J.; Efstathiou, E.; Vazquez, E.S. Activation of β-Catenin Signaling in Androgen Receptor–Negative Prostate Cancer Cells. *Clinical cancer research* **2012**, *18*, 726-736.
46. Ray, M.; Rai, N.; Jana, K.; Ghatak, S.; Basu, A.; Mustafi, S.B.; Raha, S. Beta catenin is degraded by both caspase-3 and proteasomal activity during resveratrol-induced apoptosis in HeLa cells in a GSK3β-independent manner. **2015**.
47. Sehouli, J.; Senyuva, F.; Fotopoulou, C.; Neumann, U.; Denkert, C.; Werner, L.; Gülten, O.Ö. Intra - abdominal tumor dissemination pattern and surgical outcome in 214 patients with primary ovarian cancer. *Journal of surgical oncology* **2009**, *99*, 424-427.
48. Amawi, H.; Hussein, N.A.; Karthikeyan, C.; Manivannan, E.; Wisner, A.; Williams, F.E.; Samuel, T.; Trivedi, P.; Ashby Jr, C.R.; Tiwari, A.K. HM015k, a Novel Silybin Derivative, Multi-Targets Metastatic Ovarian Cancer Cells and Is Safe in Zebrafish Toxicity Studies. *Frontiers in pharmacology* **2017**, *8*, 498.
49. Amawi, H.; Hussein, N.A.; Ashby Jr, C.R.; Alnafisah, R.; Sanglard, L.M.; ELANGOVAN, M.; Chandrabose, K.; Trivedi, P.; Eisenmann, K.M.; Robey, R.R. Bax/tubulin/epithelial-mesenchymal pathways determine the efficacy of silybin analog HM015k in colorectal cancer cell growth and metastasis. *Frontiers in pharmacology* **2018**, *9*, 520.
50. Özhan, G.; Sezgin, E.; Wehner, D.; Pfister, A.S.; Kühl, S.J.; Kagermeier-Schenk, B.; Kühl, M.; Schwille, P.; Weidinger, G. Lypd6 enhances Wnt/β-catenin signaling by promoting Lrp6 phosphorylation in raft plasma membrane domains. *Developmental cell* **2013**, *26*, 331-345.

51. Orian-Rousseau, V.; Schmitt, M. CD44 regulates Wnt signaling at the level of LRP6. *Molecular & cellular oncology* **2015**, *2*, e995046.
52. Garg, B.; Giri, B.; Majumder, K.; Dudeja, V.; Banerjee, S.; Saluja, A. Modulation of post-translational modifications in β-catenin and LRP6 inhibits Wnt signaling pathway in pancreatic cancer. *Cancer letters* **2017**, *388*, 64-72.
53. Kim, P.J.; Park, J.Y.; Kim, H.G.; Cho, Y.M.; Go, H. Dishevelled segment polarity protein 3 (DVL3): a novel and easily applicable recurrence predictor in localised prostate adenocarcinoma. *BJU international* **2017**, *120*, 343-350.
54. Gao, S.; Bajrami, I.; Verrill, C.; Kigozi, A.; Ouaret, D.; Aleksic, T.; Asher, R.; Han, C.; Allen, P.; Bailey, D. Dsh homolog DVL3 mediates resistance to IGFIR inhibition by regulating IGF-RAS signaling. *Cancer research* **2014**, *74*, 5866-5877.
55. Conacci-Sorrell, M.; Zhurinsky, J.; Ben-Ze'ev, A. The cadherin-catenin adhesion system in signaling and cancer. *The Journal of clinical investigation* **2002**, *109*, 987-991.
56. Zhao, S.; Kurenbekova, L.; Gao, Y.; Roos, A.; Creighton, C.; Rao, P.; Hicks, J.; Man, T.; Lau, C.; Brown, A. NKD2, a negative regulator of Wnt signaling, suppresses tumor growth and metastasis in osteosarcoma. *Oncogene* **2015**, *34*, 5069.
57. Dong, Y.; Cao, B.; Zhang, M.; Han, W.; Herman, J.G.; Fuks, F.; Zhao, Y.; Guo, M. Epigenetic silencing of NKD2, a major component of Wnt signaling, promotes breast cancer growth. *Oncotarget* **2015**, *6*, 22126.
58. Hu, T.; Li, C.; Cao, Z.; Van Raay, T.J.; Smith, J.G.; Willert, K.; Solnica-Krezel, L.; Coffey, R.J. Myristoylated Naked2 antagonizes Wnt-β-catenin activity by degrading Dishevelled-1 at the plasma membrane. *Journal of Biological Chemistry* **2010**, *285*, 13561-13568.
59. Van Raay, T.J.; Fortino, N.J.; Miller, B.W.; Ma, H.; Lau, G.; Li, C.; Franklin, J.L.; Attisano, L.; Solnica-Krezel, L.; Coffey, R.J. Naked1 antagonizes Wnt signaling by preventing nuclear accumulation of β-catenin. *PloS one* **2011**, *6*, e18650.
60. Jia, Y.; Cao, B.; Yang, Y.; Linghu, E.; Zhan, Q.; Lu, Y.; Yu, Y.; Herman, J.G.; Guo, M. Silencing NKD2 by promoter region hypermethylation promotes gastric cancer invasion and metastasis by up-regulating SOX18 in human gastric cancer. *Oncotarget* **2015**, *6*, 33470.
61. Chae, S.W.; Sohn, J.H.; Kim, D.-H.; Choi, Y.J.; Park, Y.L.; Kim, K.; Cho, Y.H.; Pyo, J.-S.; Kim, J.H. Overexpressions of Cyclin B1, cdc2, p16 and p53 in human breast cancer: the clinicopathologic correlations and prognostic implications. *Yonsei medical journal* **2011**, *52*, 445-453.
62. Aaltonen, K.; Amini, R.-M.; Heikkilä, P.; Aittomäki, K.; Tamminen, A.; Nevanlinna, H.; Blomqvist, C. High cyclin B1 expression is associated with poor survival in breast cancer. *British journal of cancer* **2009**, *100*, 1055.
63. Han, J.-H.; Lee, J.; Jeon, S.-J.; Choi, E.-S.; Cho, S.-D.; Kim, B.-Y.; Kim, D.-J.; Park, J.-H.; Park, J.-H. In vitro and in vivo growth inhibition of prostate cancer by the small molecule imiquimod. *International journal of oncology* **2013**, *42*, 2087-2093.
64. Fang, Y.; Liang, X.; Jiang, W.; Li, J.; Xu, J.; Cai, X. Cyclin b1 suppresses colorectal cancer invasion and metastasis by regulating e-cadherin. *PLoS One* **2015**, *10*, e0126875.
65. Androic, I.; Krämer, A.; Yan, R.; Rödel, F.; Gätje, R.; Kaufmann, M.; Strebhardt, K.; Yuan, J. Targeting cyclin B1 inhibits proliferation and sensitizes breast cancer cells to taxol. *BMC cancer* **2008**, *8*, 391.

66. Calvisi, D.F.; Conner, E.A.; Ladu, S.; Lemmer, E.R.; Factor, V.M.; Thorgeirsson, S.S. Activation of the canonical Wnt/β-catenin pathway confers growth advantages in c-Myc/E2F1 transgenic mouse model of liver cancer. *Journal of hepatology* **2005**, *42*, 842-849.
67. Brabletz, T.; Herrmann, K.; Jung, A.; Faller, G.; Kirchner, T. Expression of nuclear β-catenin and c-myc is correlated with tumor size but not with proliferative activity of colorectal adenomas. *The American journal of pathology* **2000**, *156*, 865-870.
68. Heerboth, S. Housman g, leary m, longacre m. *Byler S, lapinska K, Willbanks a and Sarkar S: emt and tumor metastasis. clin transl med* **2015**, *4*, 6.
69. Arias, A.M. Epithelial mesenchymal interactions in cancer and development. *Cell* **2001**, *105*, 425-431.
70. David, J.M.; Rajasekaran, A.K. Dishonorable discharge: the oncogenic roles of cleaved E-cadherin fragments. *Cancer research* **2012**, *72*, 2917-2923.
71. Huber, M.A.; Kraut, N.; Beug, H. Molecular requirements for epithelial–mesenchymal transition during tumor progression. *Current opinion in cell biology* **2005**, *17*, 548-558.
72. Amawi, H.; Ashby, C.R.; Samuel, T.; Peraman, R.; Tiwari, A.K. Polyphenolic nutrients in cancer chemoprevention and metastasis: Role of the epithelial-to-mesenchymal (EMT) pathway. *Nutrients* **2017**, *9*, 911.
73. Amawi, H.; Hussein, N.A.; Ashby, C.R., Jr.; Alnafisah, R.; Sanglard, L.M.; Manivannan, E.; Karthikeyan, C.; Trivedi, P.; Eisenmann, K.M.; Robey, R.W., et al. Bax/Tubulin/Epithelial-Mesenchymal Pathways Determine the Efficacy of Silybin Analog HM015k in Colorectal Cancer Cell Growth and Metastasis. *Front Pharmacol* **2018**, *9*, 520, doi:10.3389/fphar.2018.00520.
74. Manivannan, E.; Amawi, H.; Hussein, N.; Karthikeyan, C.; Fetcenko, A.; Moorthy, N.H.N.; Trivedi, P.; Tiwari, A.K. Design and discovery of silybin analogues as antiproliferative compounds using a ring disjunctive–Based, natural product lead optimization approach. *European journal of medicinal chemistry* **2017**, *133*, 365-378.
75. Hussein, N.; Amawi, H.; Karthikeyan, C.; Hall, F.S.; Mittal, R.; Trivedi, P.; Ashby Jr, C.R.; Tiwari, A.K. The dopamine D3 receptor antagonists PG01037, NGB2904, SB277011A, and U99194 reverse ABCG2 transporter-mediated drug resistance in cancer cell lines. *Cancer letters* **2017**, *396*, 167-180.
76. Karthikeyan, C.; Amawi, H.; Viana, A.G.; Sanglard, L.; Hussein, N.; Saddler, M.; Ashby, C.R., Jr.; Moorthy, N.; Trivedi, P.; Tiwari, A.K. lH-Pyrazolo[3,4-b]quinolin-3-amine derivatives inhibit growth of colon cancer cells via apoptosis and sub G1 cell cycle arrest. *Bioorg Med Chem Lett* **2018**, *28*, 2244-2249, doi:10.1016/j.bmcl.2018.05.045.
77. Albini, A.; Dell'Eva, R.; Vene, R.; Ferrari, N.; Buhler, D.R.; Noonan, D.M.; Fassina, G. Mechanisms of the antiangiogenic activity by the hop flavonoid xanthohumol: NF-kappaB and Akt as targets. *FASEB J* **2006**, *20*, 527-529, doi:10.1096/fj.05-5128fje.